Supplemental Material

Phosphatidylserine-induced Factor Xa Dimerization and Binding to Factor Va Are Competing Processes in Solution

Rinku Majumder[1], Tilen Koklic[2], Alireza R. Rezaie[3] and Barry.R.Lentz[1*]

Models and Parameter Values

A: MODEL 1: Simple Xa dimer - XaVa competition

The simplest model describing factor Xa dimerization and binding to factor Va in solution is based on the hypothesis that, in the presence of water-soluble C6PS, FXa and FVa can exist in four forms: monomers of either FXa or FVa, FXa dimer, and as a prothrombinase - FXaFVa complex. Due to high concentration of C6PS all protein species are saturated with C6PS. Because the FXa dimer is $10^6 - 10^7$ fold less active than the monomer [1], the observed rate is essentially the sum of only two rates:

$$R = [Xa_{free}] \cdot R_{Xa} + [XaVa] \cdot R_{XaVa}, \qquad \text{A1}$$

where R_{Xa} represents the rate of IIa formation by FXa in solution, whereas R_{XaVa} is the rate of IIa formation by FXaFVa complex in solution. $k_{cat}/K_{M\ Xafree}$ of thrombin (IIa) formation from II as catalyzed by free FXa in solution is 13600 $M^{-1}s^{-1}$, as determined previously[2]. We know $k_{cat}/K_{M\ XaVa}$ of prothrombinase is ~ 10^8 $M^{-1}s^{-1}$ for human prothrombinase in solution[3], but its exact value can vary slightly with protein source (*i.e.* natural versus recombinant, species, *etc*.) so we treat it as an adjustable parameter in our calculations.

---

[1] Chattopadhyay, R., et al., *Functional and Structural Characterization of Factor Xa Dimer In Solution.* Biophysical Journal, 2009. **96**(3): p. 974-986.

[2] Majumder, R., J. Wang, and B.R. Lentz, *Effects of Water Soluble Phosphotidylserine on Bovine Factor X(a): Functional and Structural Changes Plus Dimerization.* Biophys J, 2003. **84**(2): p. 1238-51.

[3] Majumder, R., G. Weinreb, and B.R. Lentz, *Efficient thrombin generation requires molecular phosphatidylserine, not a membrane surface*. Biochemistry, 2005. **44**(51): p. 16998-7006.

The process that forms these four species involves two reactions, dimerization of FXa, and prothrombinase complex formation:

$$\begin{aligned} Xa_{free} + Xa_{free} &\underset{\alpha_2}{\overset{\alpha_1}{\rightleftarrows}} Xa_2 \\ Xa_{free} + Va_{free} &\underset{\varepsilon_2}{\overset{\varepsilon_1}{\rightleftarrows}} XaVa \end{aligned}, \qquad \text{A2}$$

where Xa_{free} is FXa monomer, Va_{free} is FVa monomer, Xa_2 is FXa dimer, and XaVa is prothrombinase complex. We assume that these equilibria are established rapidly and that all protein species are in equilibrium during our measurements. Thus,

$$[Xa_2]K_d^{Xa_2} = [Xa]^2 \qquad \text{A3}$$

$$[XaVa]K_d^{XaVa} = [Xa][Va]. \qquad \text{A4}$$

Since the total concentrations of FXa and FVa are conserved, we can write two conservation equations:

$$\begin{aligned} [Xa_{tot}] &= [Xa_{free}] + 2[Xa_2] + [XaVa] \\ [Va_{tot}] &= [Va_{free}] + [XaVa] \end{aligned} \qquad \text{A5}$$

Equations A3, A4 and A5 represent a set of four equations with four unknown protein species: $[Xa_{free}], [Va_{free}], [Xa_2], and\ [XaVa]$. The set of equations was solved numerically using the "fsolve" function of MATLAB, version R2011b (7.13.0.564; Mathworks, Inc, Natick, MA).

With the concentrations of all four protein species known, Eq. 1A provides activation rates that can be compared to experimental rates (R_{obs}) to obtain R_{XaVa}, and K_d^{XaVa} by minimizing the square deviation of predicted activation rate R_{calc} from the experimental R_{obs}. Dividing by the number of degrees of freedom (#data points - #parameters -1) yields the reduced chi squared, $\overline{\chi^2}$ and parameter values in Table S1. The fit for this model is given in Figure 1 (dashed line) of the manuscript.

Table S1: Summary of all models at 5 mM Ca^{2+}

for all models: $K_{d\ Xa2}$ = 14 nM , $k_{cat}/K_{M\ Xa}$ = 1.36 10^4 $M^{-1}s^{-1}$	**K_d (nM)**	**k_{cat}/K_M ($M^{-1}s^{-1}$)**

parameter / model	$\bar{\chi}^2$ (α)	$K_{d\ XaVa}$	$K_{d\ aggregate}$	$k_{cat}/K_{M\ XaVa}$
1) Simple Xa dimer - XaVa competition	**1.38 (0.1)**	**0.32**	**/**	**$9.8\ 10^7$**
2) Xa tetramer aggregate $4Xa_{free} \rightleftarrows Xa_4$	**1.39 (0.1)**	**0.32**	**$9.8\ 10^3$**	**$9.8\ 10^7$**
2a) Sequential Xa tetramer $Xa_2 + Xa_2 \rightleftarrows Xa_4$	**1.41 (0.09)**	**0.32**	**$> 10^3$**	**$9.8\ 10^7$**
3) Va dimer $Va_{free} + Va_{free} \rightleftarrows Va_2$	**1.01 (0.45)**	**0.016**	**10^{-3}**	**$11.2\ 10^7$**
4) Xa_2Va_2 sequential aggregate $Xa_2 + Va_2 \rightleftarrows Xa_2Va_2$	**0.76 (0.78)**	**0.02**	$K_{dXa2Va2}$ = **2.7** K_{dVa2} =**0.002**	**$12.6\ 10^7$**
5) Xa_2Va_2 aggregate $2Xa_{free} + 2Va_{free} \rightleftarrows Xa_2Va_2$	**1.14 (0.29)**	**0.43**	**28**	**$11\ 10^7$**
5a) Xa_2Va_2 aggregate from the complex $2XaVa \rightleftarrows (XaVa)_2$	**1.14 (0.29)**	**0.43**	**150**	**$11\ 10^7$**

The probability (α) associated with the chi-squared distribution is defined in Statistics and Error Analysis.

B: **MODEL 2: Xa tetramer aggregate (** $4Xa_{free} \rightleftarrows Xa_4$ **)**

Because dimer formation underestimated the extent of inhibition, we considered the possibility that FXa might form a higher order aggregate, *e.g.*, a tetramer. Another model therefore assumes, in addition to assumptions in the simplest model 1, also that formation of a Xa aggregate, consisting of four Xa monomers is possible:

$$Xa_{free} + Xa_{free} + Xa_{free} + Xa_{free} \underset{\delta_2}{\overset{\delta_1}{\rightleftarrows}} Xa_4, \qquad \text{B1}$$

where Xa_4 is FXa tetramer aggregate. Thus, in addition to equations A3 and A4, following relationships applies: $[Xa_4]K_d^{Xa_4} = [Xa]^4$ B2

Assuming that the aggregate is inactive, the observed rate is then same as in equation A1.

Since the total concentration of FXa and FVa are conserved, we can write two conservation equations:

$$\begin{aligned}[Xa_{tot}] &= [Xa_{free}] + 2[Xa_2] + [XaVa] + 4[Xa_4] \\ [Va_{tot}] &= [Va_{free}] + [XaVa]\end{aligned} \quad . \qquad \text{B3}$$

Resulting set of five equations were solved numerically, similarly as in the case of model 1, with results given in Table S1. The table reveals that Model 2 provided no improvement in data description despite requiring an additional adjustable parameter ($K_d^{Xa_4}$). Indeed, the best-fit value of $K_d^{Xa_4}$ guarantees that an imperceptible amount of FXa would be present as a tetramer and, thus all other best fit parameter values were identical to those obtained with the simple dimer competition model. As a control, we tried an alternative form of the "FXa tetramer" model (Model 2a**)**

C: MODEL 2a: Sequential Xa tetramer ($Xa_2 + Xa_2 \rightleftarrows Xa_4$ **)**

This treatment is thermodynamically equivalent to the Xa tetramer aggregate model (Model 2) described above in that it differs only in the path taken to reach the tetramer species, a parameter that does not influence thermodynamic properties. Nonetheless, we analyzed it to test whether our analysis was capable of producing a thermodynamically correct result.

Additional equilibrium, as compared to the simplest model 1, describes the process of sequential tetramer formation: $Xa_2 + Xa_2 \underset{\beta_2}{\overset{\beta_1}{\rightleftarrows}} Xa_4$, C1

where Xa_2 is FXa dimer, and Xa_4 is FXa sequential tetramer aggregate. Thus,

$$[Xa_4]K_{d,seq}^{Xa_4} = [Xa_2]^2 \quad . \qquad \text{C2}$$

Conservation conditions give: $\begin{aligned}[Xa_{tot}] &= [Xa_{free}] + 2[Xa_2] + [XaVa] + 4[Xa_4] \\ [Va_{tot}] &= [Va_{free}] + [XaVa]\end{aligned}$. C3

The set of five equations with five unknown protein species was again solved numerically as described under Model 1, with results given in Table S1.

It is easy to see that:

$$K_{d,seq}^{Xa_4} = [Xa_2]^2 \Big/ [Xa_4] = [Xa]^4 \Big/ (K_d^{Xa_2})^2 [Xa_4] = [Xa_4] K_{d,a}^{Xa4} \Big/ (K_d^{Xa_2})^2 [Xa_4] = K_{d,a}^{Xa4} \Big/ (K_d^{Xa_2})^2 , \qquad \text{C4}$$

so $K_{d,seq}^{Xa_4}$ is defined in terms of $K_{d,seq}^{Xa_4}$ and $K_d^{Xa_2}$. From Table S1, we see that $K_{d,seq}^{Xa_4} \approx 10^4$ and $K_d^{Xa_2} = 14$, so the value of $K_{d,a}^{Xa_4}$ is just as predicted from thermodynamics. All other parameters obtained with the models 2 and 2a (Table S1) are identical, confirming that the analysis method used to describe our data provides results consistent with thermodynamics. Because of the thermodynamic equivalence, the fit was identical to that obtained with the Xa tetramer aggregate ($4Xa_{free} \rightleftarrows Xa_4$) (model 2). This allows us to reject the "higher-order Xa aggregate" (as embodied to a first approximation in a tetramer) model to explain inhibition observed at higher concentrations of FXa.

D: MODEL 3: Va dimer ($Va_{free} + Va_{free} \rightleftarrows Va_2$)

Next, we considered whether aggregation of FVa might contribute to the less than satisfactory quantitative description we had obtained using the dimer competition model (model 1).

This treatment is based on an additional assumption, compared to the simplest model 1, that FVa can form dimers:

$$Va_{free} + Va_{free} \underset{\varphi_2}{\overset{\varphi_1}{\rightleftarrows}} Va_2 , \qquad \text{D1}$$

where Va_{free} is FVa monomer, and Va_2 is FVa dimer, resulting in additional relationship:

$$[Va_2] K_d^{Va_2} = [Va_{free}]^2 \quad , \qquad \text{D2}$$

and modified conservation equation regarding FVa:

$$[Va_{tot}] = [Va_{free}] + 2[Va_2] + [XaVa] . \qquad \text{D3}$$

We fit this model to the data similarly as described for model 1, to obtain the parameters in Table S1. Reference to Table S1 reveals that this model provided slightly lower $\overline{\chi^2}$ and a somewhat higher α value (0.45), but the appearance of the fit was essentially unchanged and the parameter values were

quite unreasonable relative to other reports (K_d^{XaVa} = 0.016 nM relative to the reported 0.6 nM [4] or to common sense ($K_d^{Va_2}$ = 1 pM means that FVa binds to FVa 100 times more tightly than it does to FXa). If this were true, we should see clear evidence of FVa dimer in native gels of mixtures of FVa and FXa in the presence of C6PS (Figure 3). For these reasons, we conclude that aggregation of FVa cannot offer an explanation for the poor quantitative agreement between the FXa dimer competition model and our data.

E: MODEL 4: Xa_2Va_2 sequential aggregate ($Xa_2 + Va_2 \rightleftarrows Xa_2Va_2$)

Next we considered whether, if FVa formed a dimer, it might interact with FXa dimer to form an aggregated FXaFVa complex. This treatment is based on additional hypothesis, compared to the simplest model 1, that FXa and FVa exist as FVa dimer, and as Xa_2Va_2 aggregate, consisting of Xa and Va dimers, as described by the following two additional equiliria:

$$\begin{aligned} Va_{free} + Va_{free} &\underset{\varphi_2}{\overset{\varphi_1}{\rightleftarrows}} Va_2 \\ Xa_2 + Va_2 &\underset{\nu_2}{\overset{\nu_1}{\rightleftarrows}} Xa_2Va_2 \end{aligned}, \qquad \text{E1}$$

where Va_{free} is FVa monomer, Xa_2 is FXa dimer, Va_2 is FVa dimer, and Xa_2Va_2 is the aggregate consisting of a FXa dimer and FVa dimer, which results in two additional equations:

$$[Va_2]K_d^{Va_2} = [Va_{free}]^2 \qquad \text{E2}$$

$$[Xa_2Va_2]K_d^{Xa_2Va_2} = [Xa_{free}]^2[Va_{free}]^2, \qquad \text{E3}$$

and modified conservation equations:

$$\begin{aligned} [Xa_{tot}] &= [Xa_{free}] + 2[Xa_2] + [XaVa] + 2[Xa_2Va_2] \\ [Va_{tot}] &= [Va_{free}] + 2[Va_2] + [XaVa] + 2[Xa_2Va_2] \end{aligned}. \qquad \text{E4}$$

Assuming that the Xa_2Va_2 aggregate is inactive, the rate is again the sum of two rates as in model 1.

[4] Majumder, R., et al., *A phosphatidylserine binding site in factor Va C1 domain regulates both assembly and activity of the prothrombinase complex.* Blood, 2008. **112**(7): p. 2795-802.

This model yields a set of six equations, which was solved numerically as described for model 1, to obtain the parameters in Table S1. We see from the Table S1 that including this possibility improved the quantitative description of our data considerably, except at the lowest FVa concentrations and highest FXa concentrations, when residuals remained considerable (data not shown). Of course, this treatment required four adjustable parameters ($K_d^{V_{a_2}}; K_d^{V_a X_a}; K_d^{Xa_2 Xa_2}; (k_{cat}/K_M)_{XaVa}$, *i.e.*, one more than any other model we consider, because it considers an additional species ($Va_{,\,dimer}$). While it provided a better quantitative description (lower $\overline{\chi^2}$ and larger α, Table S1) and a better appearing fit to the data (data not shown), this improvement is discounted by the need for an additional adjustable parameter, the presence of which in a model generally provides a lower $\overline{\chi^2}$. As for Model 3, the value of $K_d^{Va_2}$ was also physically unreasonable. Thus, we must also reject this model.

F: MODEL 5: Xa_2Va_2 aggregate ($2Xa_{free} + 2Va_{free} \rightleftarrows Xa_2Va_2$ **)**

Finally, we considered whether dimerization of the XaVa complex might help account for our data. In this, we treated two thermodynamically equivalent versions of this model (Models 5 and 5a). The first model is based on the hypothesis that FXa and FVa can also exist as Xa_2Va_2 aggregate, formed directly from Xa and Va monomers. As in Model 4, we assume the Xa_2Va_2 aggregate is inactive. The process that forms such aggregate involves the additional equilibrium:

$$Xa_{free} + Xa_{free} + Va_{free} + Va_{free} \underset{\xi_2}{\overset{\xi_1}{\rightleftarrows}} Xa_2Va_2, \qquad \text{F1}$$

where Xa_{free} is FXa monomer, Va_{free} is FVa monomer, and Xa_2Va_2 is the aggregate. This results in just one additional equation, as compared to the simplest model 1:

$$[Xa_2Va_2]K_d^{Xa_2Va_2} = [Xa_{free}]^2[Va_{free}]^2 \qquad \text{F2}$$

and modified conservation equations:

$$\begin{aligned}[Xa_{tot}] &= [Xa_{free}] + 2[Xa_2] + [XaVa] + 2[Xa_2Va_2] \\ [Va_{tot}] &= [Va_{free}] + [XaVa] + 2[Xa_2Va_2]\end{aligned}. \qquad \text{F3}$$

This set of equations was solved numerically as described above, to obtain the parameters in Table S1.

G: MODEL 5a: Xa_2Va_2 aggregate from the complex ($XaVa + XaVa \rightleftarrows (XaVa)_2$)

The second thermodynamically equivalent model is based on the hypothesis that FXa and FVa can form Xa_2Va_2 aggregate, consisting of 2 FXaFVa complexes. Again, we assume that the aggregate is inactive.

The additional equilibrium involved is: $2(XaVa) \underset{\nu_2}{\overset{\nu_1}{\rightleftarrows}} (XaVa)_2$, G1

where XaVa is prothrombinase complex, and $(XaVa)_2$ is the Xa_2Va_2 aggregate consisting of two FXaFVa complexes, with equilibrium constant: $[(XaVa)_2]K_d^{(XaVa)_2} = [XaVa]^2$ G2

Proceeded as previously described we obtain the parameters in Table S1. As for Model 2, we wished to check whether analysis of thermodynamically equivalent models led to equivalent results. As seen in Table S1 (note $K_d^{(XaVa)_2} = K_d^{Xa_2Va_2} / \left(K_d^{XaVa}\right)^2$ if $(XaVa)_2 = Xa_2Va_2$), the results for these two models are equivalent, as anticipated. The $\overline{\chi^2}$ for this model is lower than any except that of Model 4, for which there are four instead of three adjustable parameters and for which the predicted value of $K_d^{Va_2}$ was completely physically unreasonable. The description of our data by this model is better than for any other model considered (*i.e.*, lowest $\overline{\chi^2}$ for physically reasonable parameters; Table S1). The parameters for this model (K_d^{XaVa};$(k_{cat} / K_M)_{XaVa}$) were also in reasonable agreement with literature estimates [5], while the predicted $K_d^{(XaVa)_2}$ (150 nM) is consistent with our failure to observe this species in native gels (Figure 3).

[5] Majumder, R., G. Weinreb, and B.R. Lentz, *Efficient thrombin generation requires molecular phosphatidylserine, not a membrane surface.* Biochemistry, 2005. **44**(51): p. 16998-7006.

Statistics & Error Analysis

We must first determine a measure of goodness of fit. While there are several ways to accomplish this, we choose a very simple one associated with the chi-squared test. It uses the sum of squared differences between the observed (experimental) and expected outcome (predicted by a theoretical model) each divided by measurement error of each experimental data point as a measure of goodness of fit:

$$\chi^2 = \sum_{i=1}^{N} \frac{\left(O_i - E_i\right)^2}{\sigma_i^2}, \qquad \text{(ES1)}$$

where O_i is an experimentally observed quantity, E_i is an expected value of a quantity predicted by a model, σ_i is standard deviation of *i*-th measurement, and *N* is the number of experimental data points.

The reduced chi-squared was calculated by dividing the chi-squared by the number of degrees of freedom:

reduced chi square $$\overline{\chi^2} = \frac{1}{\nu} \sum_{i=1}^{N} \frac{\left(O_i - E_i\right)^2}{\sigma_i^2}, \qquad \text{(ES1)}$$

ν is the number of degrees of freedom $\nu = N - p - 1$, *N* is the number of experimental observations, and *p* is the number of fitted parameters. Large $\overline{\chi^2} >> 1$ indicates a poor fit, $\overline{\chi^2} > 1$ indicates that the model doesn't fully describe the experimental data, $\overline{\chi^2} \approx 1$ indicates that the model describes the data adequately, within standard deviations σ_i of experimental data points, while $\overline{\chi^2} < 1$ indicates that a model is "over-fitting" the data, which is a consequence of overestimated standard deviations σ_i due to insufficient repetitions of measurements or the model is fitting the experimental noise.

To obtain the probability associated with the chi-squared distribution (**α**) of each best fit, we used the CHIINV function in Excel (This has been replaced by CHISQ.INV function in 2010 and 2011 and later versions) along with the number of degrees of freedom for a particular experiment. Probability level α can take a value from 0 to 1. For a model going exactly through all the data points

reduced $\overline{\chi^2} = 0$ with corresponding α=1, while a model inconsistent with the experimental data $\overline{\chi^2} \to \infty$ with corresponding α=0. For a model contained within standard deviations of the experimental data (perfect fit) one gets $\overline{\chi^2} = 1$ with corresponding α=0.5. The larger the probability level or the closer the $\overline{\chi^2}$ is to 1, the more likely it is that the proposed model adequately describes the experimental data. Thus, the probability level is a measure of appropriateness of the model to describe the data. The probability levels associated with $\overline{\chi^2}$ of the best fit returned by MatLab are presented in Table S1. Accordingly to recently debated controversies in 'null hypothesis significance testing' we are comparing α's, probabilities associated with the chi-squared distribution, in order to compare different models and not to accept or reject specific hypothesis[6]. In order to provide additional certainty of proposed fitting models we compared predictions of different fitting models with previously published observations as well as other types of experiments where predictions of a model could be directly observed.

Next, we used observed $\overline{\chi^2}$ values to estimate parameter uncertainties, for each best fit parameter. They were estimated by finding fitting parameter values for which the chi-squared values are higher than the original best-fit value, but lower than a critical value ($\overline{\chi^2}_{best\ fit} < \overline{\chi^2} < \overline{\chi^2}_{critical}$), which is usually referred to as "the projections of the error surface method". In this way an interval of fitting parameter values, for which $\overline{\chi^2}_{best\ fit} < \overline{\chi^2} < \overline{\chi^2}_{critical}$, is obtained. Because MatLab determines the best fit in a non-analytical fashion, it does not return uncertainties in parameter values. Determination of these is commonly done in canned fitting routines by assuming independence of parameter uncertainties, even though these are not independent, and then derivatives of the test function in N independent parameter directions provide uncertainties. Another problem occurs when these derivatives cannot be expressed analytically. Even though these can be determined numerically

[6] Gigerenzer, G., *Mindless statistics.* The Journal of Socio-Economics, 2004. **33**: p. 587-606.

in MatLab, we have taken the approach of using MatLab to obtain an N-dimensional array of $\overline{\chi^2}$ in parameter space. In a plane of this array for which all parameters but two are fixed at minimized values, we plot iso-$\overline{\chi^2}$ lines that generally define ellipses. Extremal values of a fitting parameter corresponding to selected iso-$\overline{\chi^2}$ line, which define a confidence interval, are read from the graph. This process can be continued for additional pairs of parameters until the extrema of all parameter values are determined. These are given in Table S1. This method is described at https://delta.physics.uiowa.edu//~cak/papers/swpfit/node3.html and is illustrated below for the best fit obtained from Model 1 of the 5 mM Ca^{2+} data, as recorded in Figure 2 and Table 1.

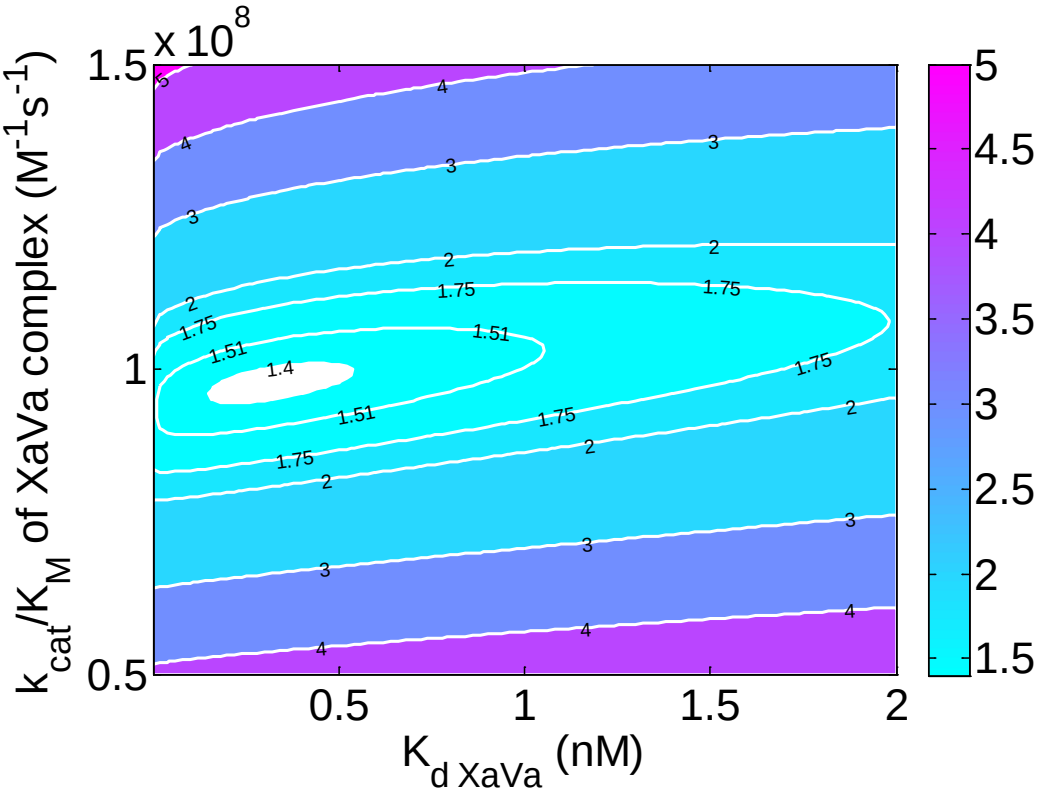

Figure S1. Chi2 versus XaVa activity and dissociation constant for Model 1 as applied to data in Figure 1 in the presence of 5 mM Ca^{2+}. The lightest blue area represents all solutions with $\overline{\chi^2} < \overline{\chi^2}_{critical} = 1.51$. The scale on the right represents values of reduced chi square. The parameter ranges given in Table S1 were obtained from such diagrams as described above. Note that the

confidence interval of k_{cat}/K_M as defined with iso-$\overline{\chi^2}$ line is fairly symmetric, while the interval of K_d is not.

Effects of R165A FXa mutation FVa Binding

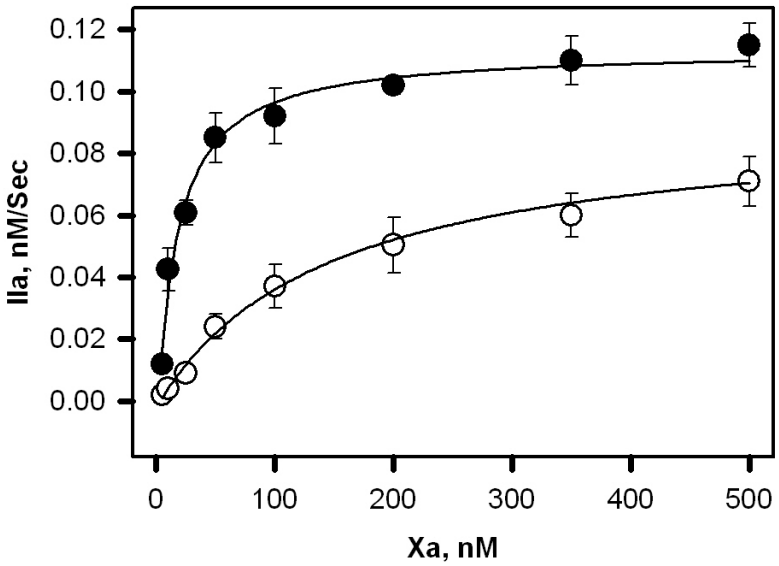

Figure S1: Prothrombin activation by increasing concentration of wild type and mutant (R165A) FXa in the presence of 400 μM C6PS and 5 mM Ca^{2+} at 37^0C: The initial rates of prothrombin activation by FXa is plotted as a function of FXa (closed circles) or mutant R165A FXa (open circles). The appearance of thrombin was determined by the rate of hydrolysis of DAPA (as described in Methods). The reaction mixture contained 1 μM prothrombin, FXa in 50 mM Tris, 175 mM NaCl, 0.6% poly(ethylene glycol), 5 mM Ca^{+2} and 400 μM C6PS. The dimerization K_d obtained in the presence of wild type and mutant FXa are 16 and 147 nM, respectively.

Protein species as predicted with the simplest model 1

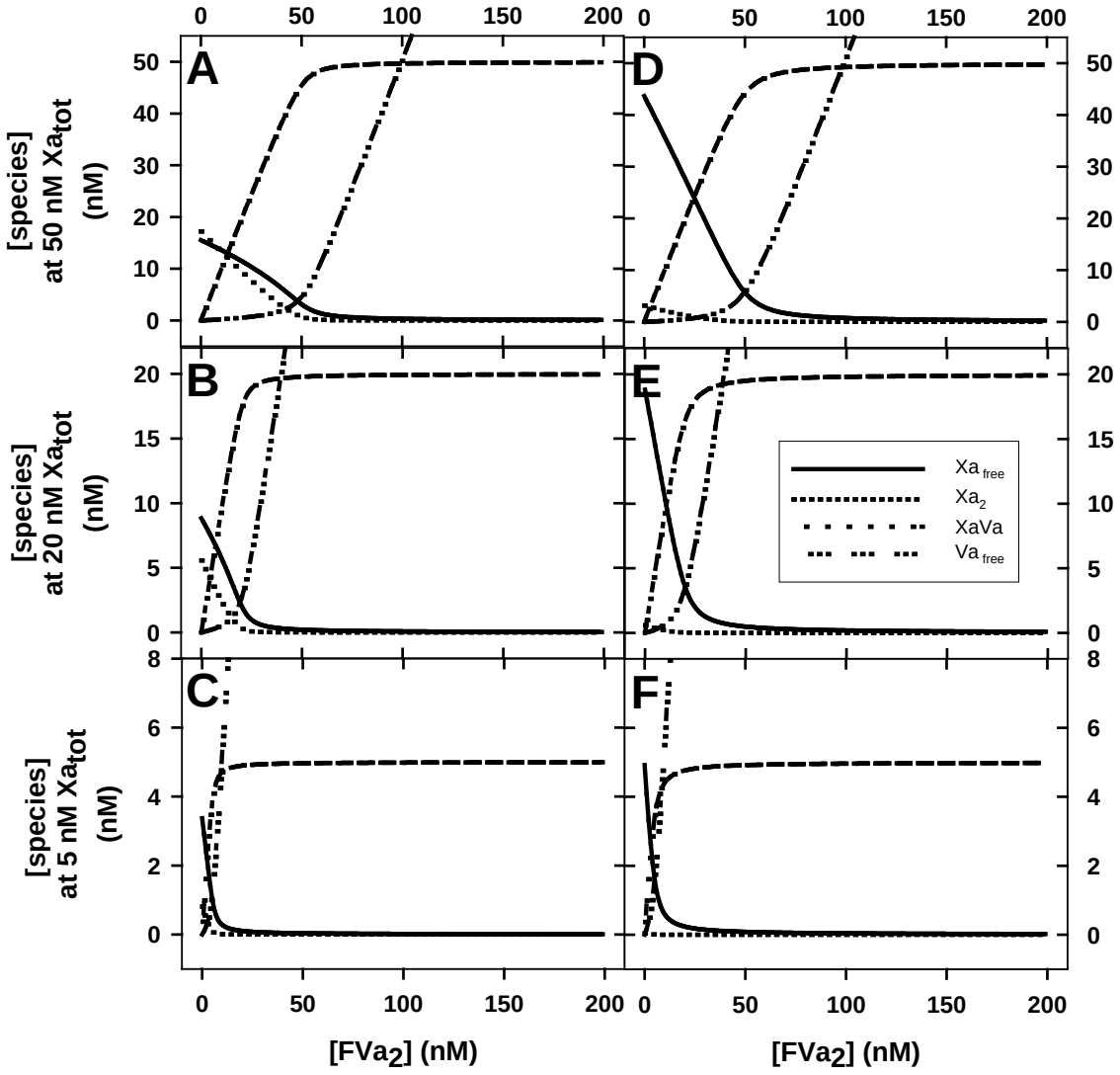

Figure S2: Simulations of protein species with the parameters obtained based on Model 1 (Simple Xa dimer - XaVa competition) as a function of added FVa. Left column: at 5mM Ca^{2+} and 5 (Frame A), 10 (Farme B), and 50 (Frame C) nM FXa; right column: at 3mM Ca^{2+} and 5 (Frame D), 10 (Farme E), and 50 (Frame F) nM FXa.

Protein species as predicted with the Model 5a

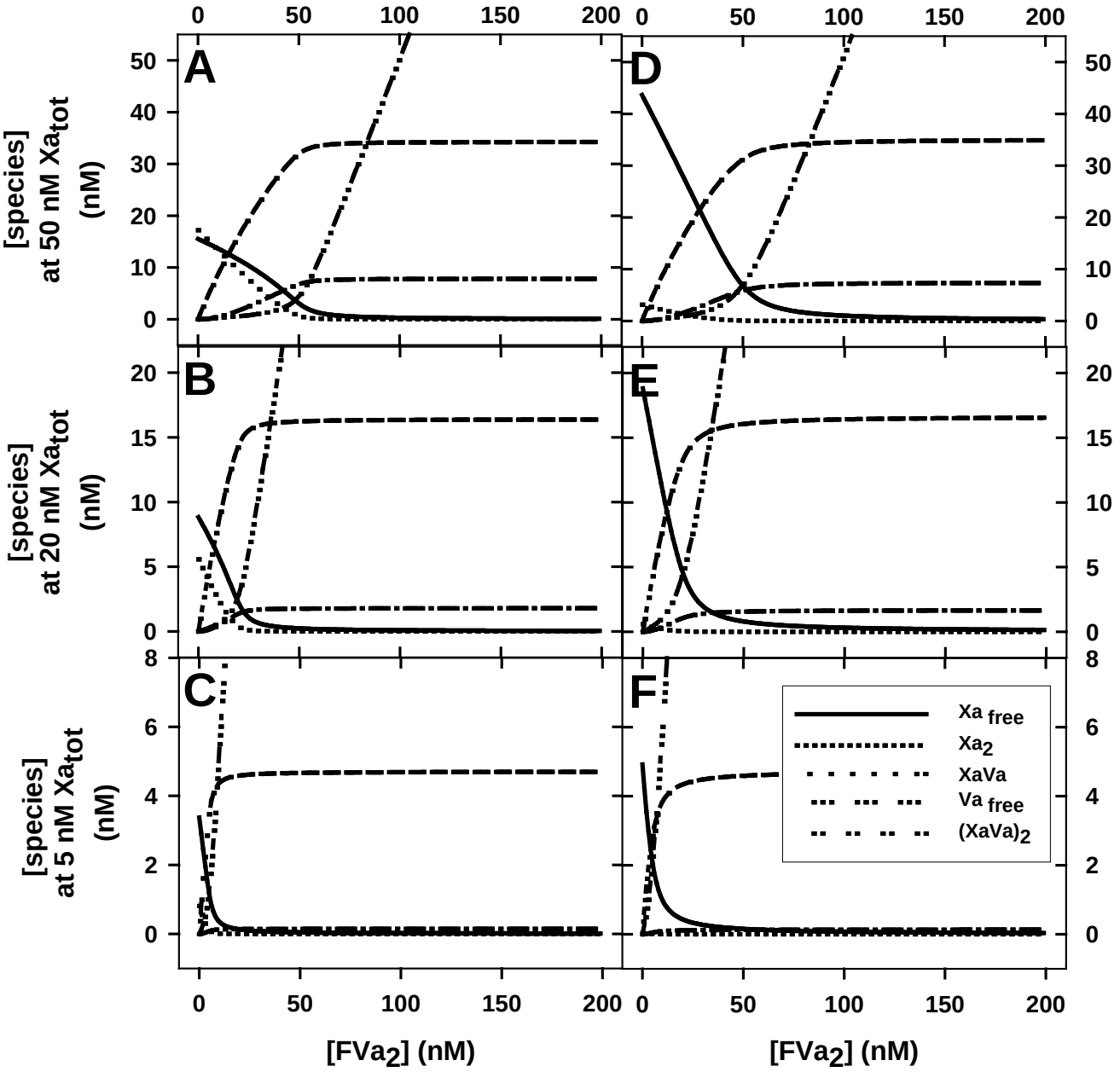

Figure S3: Simulations of protein species with the parameters obtained based on Model 5a (Xa_2Va_2 aggregate) as a function of added FVa. Left column: at 5mM Ca^{2+} and 5 (Frame A), 10 (Farme B), and 50 (Frame C) nM FXa; right column: at 3mM Ca^{2+} and 5 (Frame D), 10 (Farme E), and 50 (Frame F) nM FXa.